Polymer Degradation and Stability
February 2022, Volume 196 Pages 109848 (7p.)
https://doi.org/10.1016/j.polymdegradstab.2022.109848
https://archimer.ifremer.fr/doc/00750/86161/

Fracture test to accelerate the prediction of polymer embrittlement during aging – Case of PET hydrolysis

Arhant Mael [1, *], Le Gall Maelenn [1], Le Gac Pierre Yves [1]

[1] Marine Structures Laboratory, IFREMER, Centre de Bretagne, Plouzané, France

* Corresponding author : Mael Arhant, email address : mael.arhant@ifremer.fr

Abstract :

Depending on the nature of a given polymer and the environment, the rate of degradation can vary significantly, from a few hours up to tens of decades. In the polymer aging community, it is therefore a true challenge to obtain an understanding of the loss in properties of a given polymer within a reasonable time frame. The present work presents a novel approach to decrease that time. Within this study the decrease in mechanical properties of the polyethylene terephthalate under hydrolysis process has been followed via the Essential Work of Fracture method (EWF-m) and compared to the more classical tensile test. The degradation has been accelerated by increasing temperature, (from 60 °C up to 110 °C). Results show a rapid decrease in the non-essential work of fracture compared to the maximal stress at break obtained by tensile test. It appears that fracture properties can be used for both time/temperature superposition as well as the determination of the critical molar mass. Moreover, as fracture properties are very sensitive to degradation, it appears that it is possible to decrease aging time/temperature using EWF.

Highlights

► Fracture properties are more sensitive to chemical degradation than classical tensile properties. ► It is possible to reduce aging duration and/or temperature thanks to fracture results. ► Structure/properties relationships can be described using fracture results.

Keywords : Fracture properties, Polymer aging, Hydrolysis, Prediction, Embrittlement

1. Introduction

Polymers are widely used because of their intrinsic properties such as ease of processing, low thermal conductivity, low density and the ability to undergo large deformation [1]. One of their limitations is their durability, particularly when subjected to environmental degradation. Indeed, polymers undergo degradation over time that can be reversible (physical) or irreversible (chemical). For long term use (from 20 to 80 years), it is necessary to ensure the durability of the material over the defined time range.

The study of polymer durability is generally done over relatively short durations (usually less than 3 years), which are small compared to the duration in service. It is thus necessary to accelerate the aging. Generally, acceleration is done by increasing the aging temperatures to ensure that a loss of mechanical properties can be observed within the aging duration. It is then necessary to extrapolate from the high temperatures to the service temperature either using an empirical approach [2-4] or physical models [5-6]. The quality of this extrapolation depends on many parameters such as the number of degradation processes involved, the potential couplings between degradation processes, the homogeneous or heterogeneous character of the degradation and the temperature range used for accelerated aging [7-9]. Very high aging temperatures can lead to different degradation processes from those that will take place in service. There is therefore a trade-off between the temperature range used and the aging times involved in polymer durability studies. To overcome these limitations, highly sensitive

experimental approaches have been developed in the past with the aim to decrease aging temperatures, such as oxygen consumption [10-12] but also molar mass measurements [13-14]. The latter is particularly interesting because it is relevant for all aging processes, not only oxidation. Here, with the same purpose, we propose to use a very sensitive mechanical characterization technique at the first stage of aging, the crack propagation, coupled with molar mass measurements.

Crack growth tests consist of measuring the energy necessary to propagate an existing defect, contrary to classical tensile tests where it is considered that there is no initial defect. Interpretation of these tests can be, for polymers, complex because the energy provided to the specimen during the test is not exclusively used to propagate the crack but also for other processes such as deformation at the crack front or the appearance of plastic strain in the specimen. The concept of Essential Work of Fracture (EWF) was introduced to overcome these difficulties. It allows the dissociation of the energy essential to propagate the crack from the energy consumed by the other processes [15, 16]. This characterization method has been widely used with PET, for which many papers have been published [17-20]. An excellent review can be found in [21]. However very few studies have considered changes in crack propagation properties during chemical degradation (the work of Barany [22] for example only focused on plasticization of PET by water). Aside from PET, the study of embrittlement through EWF tests was performed by Fayolle et al. in 2004 on polypropylene [23]. In that study, tests were performed on samples with different molecular weights tested at different temperatures. From these tests, a change from ductile to brittle behaviour was identified with EWF-m but there was no comparison with tensile test results. Their work was then extended in [24] where a decrease in fracture properties (using EWF-m) was observed while no change in elongation at failure observed. Finally, another study was carried out on PTFE in [25] where the assessment of

embrittlement was made through EWF tests. These studies demonstrate that the EWF-Fracture Test Method provides an interesting tool to investigate degradation at the early stages of aging. The objective of the study proposed here is to highlight the interest of crack propagation tests in the context of polymer aging. We have chosen to illustrate this interest via the hydrolysis of PET for 3 main reasons: the chemical mechanisms of hydrolysis of PET are known in the literature [26-30], the mechanical mechanisms involved in the crack propagation test are available in the literature [21] and finally the results from tensile tests on the same material under simulated aging conditions (materials, temperature, etc...) were recently performed by the authors [31].

In this paper, a presentation of the material and techniques used in this paper will be provided first with a detailed description of the EWF concept. Second, results from EWF tests in the unaged state will be presented, followed by the effect of aging on the fracture properties investigated at one specific aging temperature (105°C). The behaviour is then generalized to other aging temperatures. Finally, it is demonstrated that the use of the EWF approach is more sensitive to aging than classical tensile tests.

2. Materials and methods

2.1. Material

A Polyethylene terephthalate (PET) manufactured by extrusion was used in this study. It is a PET grade commonly used in plastic bottles (Silar 874 C80) and was received in the form of polymer films of 200 µm thickness. It has a density of 1.37 g cm^3 and an initial crystallinity ratio of 7 %. All specimens were recrystallized thermally before aging, at 110°C (the highest aging temperature considered in this study) for 30 min until a stable crystallinity ratio was reached (X_c = 33%). This procedure leads to a thermally stable material before aging. The initial molar mass and polydispersity index were 31.4 kg/mol and 2.4 respectively.

2.2. Aging

Aging was performed in deionised water at different temperatures ranging from 60 to 110°C (60, 80, 100, 105 and 110°C). Aging conditions below 100°C were obtained in water tanks at atmospheric pressure, while those performed above 100°C were carried out using pressure vessels at a fixed pressure of 15 bars to ensure water remained liquid during aging. Following aging, samples were dried in desiccators at 0% humidity and ambient temperature until the weight was stabilized before testing.

2.3. Size Exclusion Chromatography (SEC)

Molar mass was determined using SEC by the PeakExpert Company according to the Laun and al. method [32]. Samples of 10 mg were dissolved in 4 mL of hexafluoroisopropanol (HFiP). The dissolution was performed for 24 h at room temperature. The solution was then filtered using a PTFE membrane of 0.2 µm pore size. The separation was performed using a pre-column and two columns packed with 7 ₘm PFG particles, and 1000 Å and 100 Å pore size, the dimension of columns was 8 mm ID x 300 mm length. The mobile phase was a mixture of HFiP þ 0.05 mol/L potassium tri-fluoroacetate (KTFAc), flow rate was 1 mL/min and injection volume was 50 µL. The detection was performed using a Waters 2414 differential refractive index detector and data treated with PSS WinGPC unity v7.5 SEC software. The calibration was performed using poly(methyl methacrylate) standards supplied by PSS GmbH Mainz, Germany, with molar mass ranging between 800 and 1,600,000 g/mol and the calibration curve was adjusted with a 5^{th} order polynomial. Calculations are conventional and average molecular weights are expressed as PMMA equivalents.

2.4. Fracture tests – EWF

Essential Work of Fracture (EWF) was used throughout this paper to perform fragmentation tests. This method is based on the total work of fracture (W_f), that can be divided in two components, i.e. the essential work of fracture (W_e) and the non-essential work of fracture (W_p). These two components respectively represent the inner (IPZ) and outer process zones (OPZ). If we assume that both of these zones occur within the ligament, the total work of fracture can be written as follows:

$$w_f = w_e + \beta w_p . L$$

Where w_e is the component associated with the essential work of fracture, βw_p the plastic deformation component with β the shape factor associated with the form of the outer process zone and finally L the ligament length. D-DENT specimens were used, the dimensions chosen are shown in Figure 1 and the thickness of the films was 200µm. Ligament lengths were chosen to fulfil the plane stress conditions and ranged between 5 and 15 mm. These were obtained by slitting the edges of the specimen on both ends using a sharp razor blade. Ligament lengths were measured using a Leica microscope. A minimum of 10 samples was targeted for each aging condition, however, due to the complexity in testing highly brittle D-DENT specimens after aging, some specimens were broken before testing. Therefore, for some conditions there were slightly less than 10 samples tested (for each condition, at least 7 specimens were tested). All tests were performed at 1 mm/min on an Instron testing machine using a load cell of 500 N.

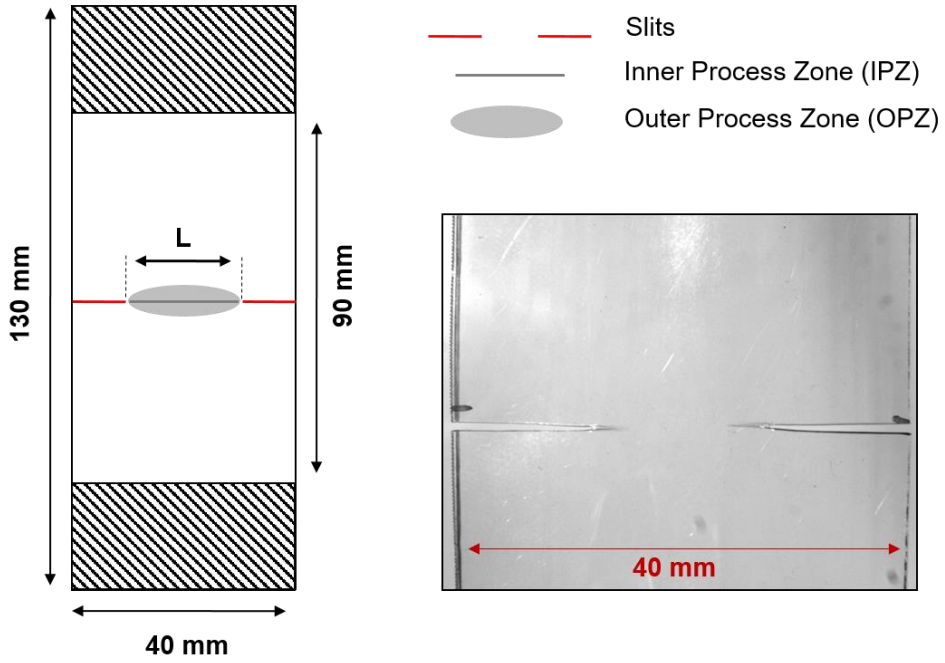

Figure 1 : Dimensions of the EWF specimens used in this study – Deeply double edge notched specimen

3. Results

3.1. Fracture properties with unaged samples

Crack propagation tests were first performed on the unaged specimens, to provide a baseline for the following tests performed after aging. First, load-displacement plots at different ligament lengths are shown in Figure 2.a. Then, the total work of fracture W_f is plotted as a function of ligament length, in order to identify the EWF parameters in the unaged state in Figure 2.b.

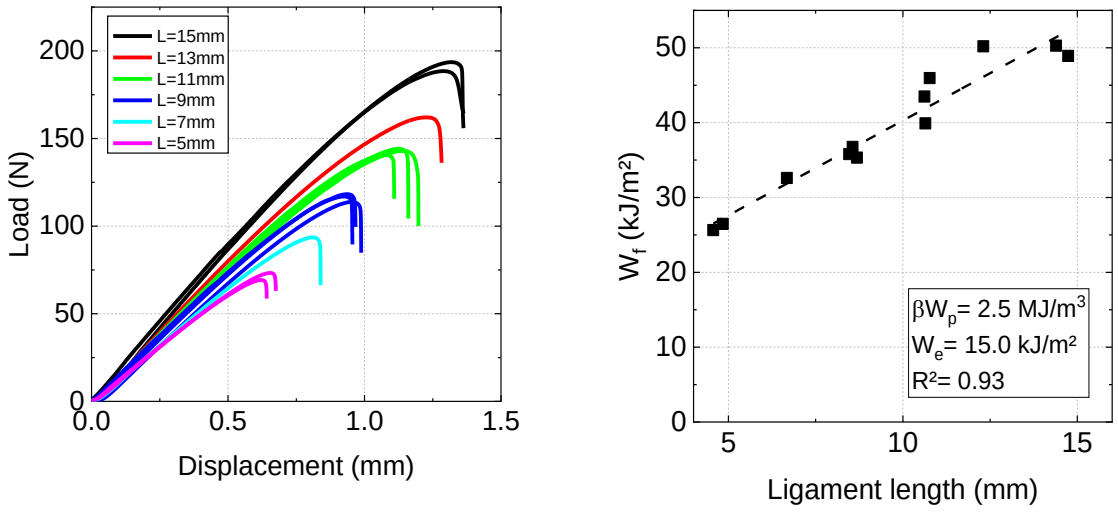

(a) **(b)**

Figure 2: EWF tests in the unaged state (a) Load-displacement plots (b) Specific essential work of fracture as a function of ligament length

Results from Figure 2.a show that as the ligament length decreases, the maximum displacements at failure and associated loads decrease accordingly. Also, the failure occurs just after ligament yielding.

Results in Figure 2b show that as the ligament length increases, W_f increases accordingly. From the slope and intercept of this plot, we are able to identify the EWF parameters, i.e., βw_p and w_e, respectively equal to 2.5 MJ/m^3 and 14.9 kJ/m².

3.2. Impact of hydrolysis on fracture properties

3.2.1. Aging at 105°C

Specimens were then aged according to the method described in 2.2., i.e. in deionised water. Here results from fracture tests performed after aging at 105°C are presented. First, load-displacement plots are shown for different aging durations on Figure 3, for a ligament length of 10 mm.

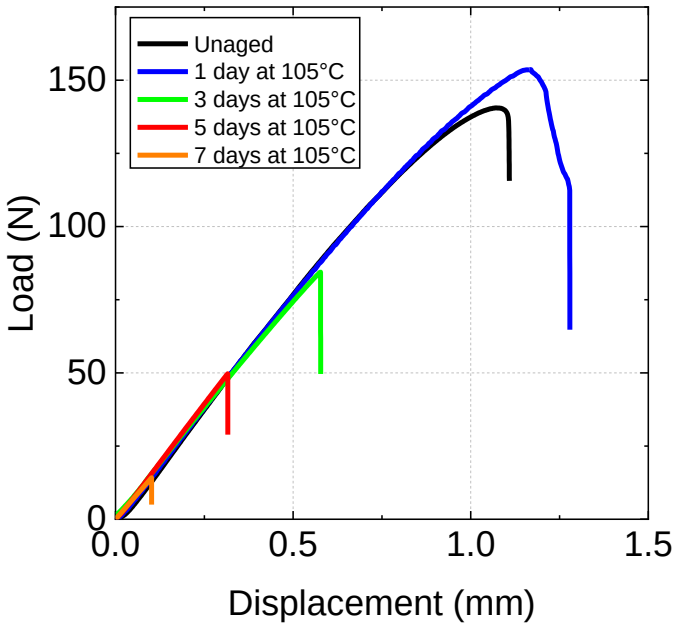

Figure 3: Load displacement plots for L=10 mm for different aging durations in water at 105°C

Figure 3 clearly demonstrates that aging in water has a significant effect on the fracture behaviour of PET. After 1 day of aging, the material experiences a slight increase in both its maximal load and displacement at failure. On the other hand, for aging durations longer than 1 day, the properties at failure are greatly decreased. Also, no ligament yielding is observed before failure while it was seen earlier with unaged samples. This shows that the material now exhibits a brittle behaviour. These results were for a ligament length of 10 mm. To generalize this behaviour, Figure 4 now compiles W_f as a function of all ligament lengths tested at this aging condition (i.e. 105°C) for different aging durations.

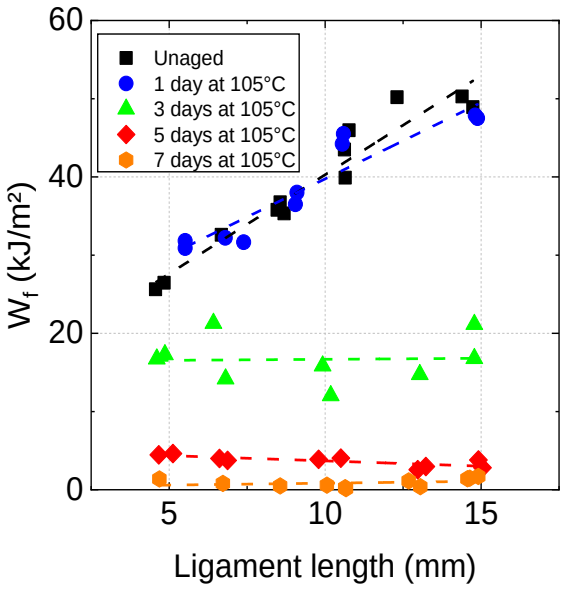

Figure 4: Effect of aging at 105°C on the fracture energy in PET

After 1 day of aging, fracture properties are fairly similar to those in the unaged state. However, for longer aging times, the slope of the curves flattens and tends to reach a value of 0. From these plots the essential (w_e) and non-essential (βw_p) work of fracture parameters are identified for each aging condition, and are respectively plotted as a function of aging time in Figure 5.a and Figure 5.b.

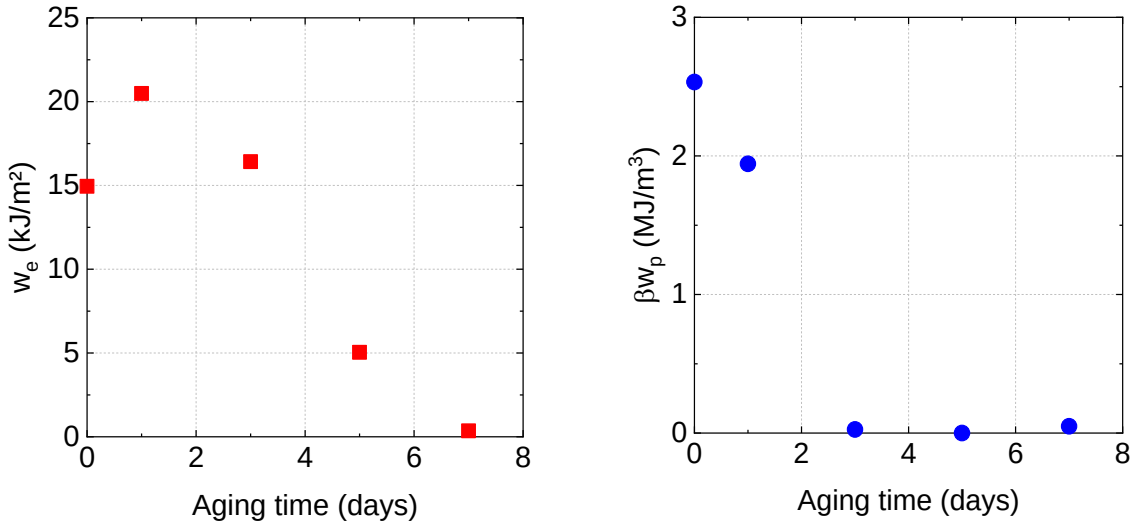

(a) **(b)**

Figure 5: Effect of aging at 105°C on EWF parameters (a) w_e (b) βw_p

Results from Figure 5.a show that the essential work of fracture parameter (w_e), which is related to the energy necessary to propagate a crack, starts to increase at the early stages of aging (from 15 kJ/m² in the unaged state up to 21 kJ/m² after 1 day at 105°C). Afterwards, for longer aging times, w_e seems to decrease linearly until it reaches zero after 7 days of aging. In Figure 5.b, the non-essential work of fracture parameter (βw_p), which is related to the energy induced by plastic deformation around the crack tip, decreases linearly from 2.5 MJ/m^3 in the unaged state down to zero after 3 days of aging. Afterwards, no further change in βw_p is observed as it stabilizes at values close to 0 MJ/m^3. These results show that aging has a significant effect on the fracture properties of PET.

If we now compare these changes in both w_e and βw_p with the decrease in maximal stress measured in tensile tests during aging at 105°C, i.e, in the same condition (see figure 6 below, from [31]), it clearly appears the aging time necessary to observe a decrease in the mechanical properties is much shorter based on fracture properties than on maximal stress.

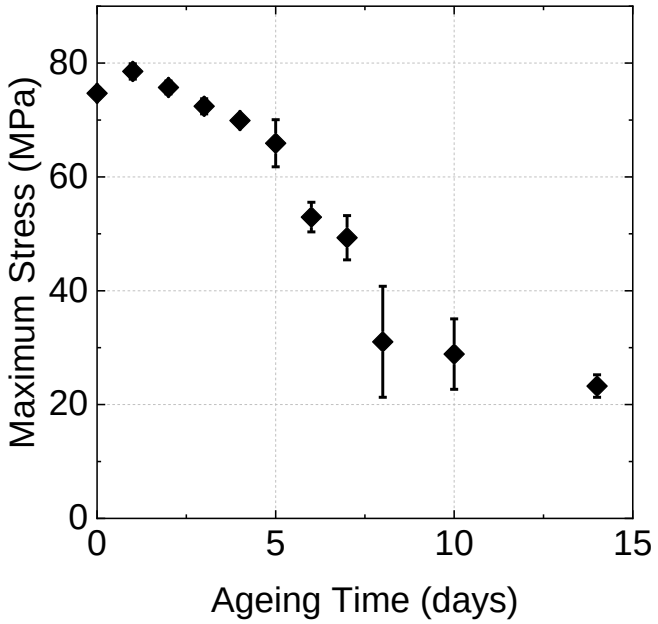

Figure 6: Maximal stress from tensile tests after aging at 105°C, from [31]

In fact, the maximal stress starts to drop after more than 5 days of aging whereas here βw_p is equal to 0 after only 3 days of aging. This means that fracture properties are more sensitive to degradation than classical tensile properties. This is of interest for the polymer aging community because it could not only significantly reduce the time needed to age samples but also allow the use of lower aging temperature for better lifetime prediction. However, it is necessary to answer two main questions.

- First, can the time/temperature extrapolation based on fracture properties be compared to that from tensile results?

- Second, is it possible to propose relationships between the macromolecular network of the polymer and its fracture properties based on EWF testing?

3.2.2. Time/Temperature superposition based on fracture properties

To answer the first question raised above, the fracture properties after aging at different temperatures are considered in the next section.

3.2.2.1. Fracture tests after aging at different temperatures

Fracture tests were performed on specimens aged at different temperatures (from 60°C up to 110°C). Results are shown in Figure 7.

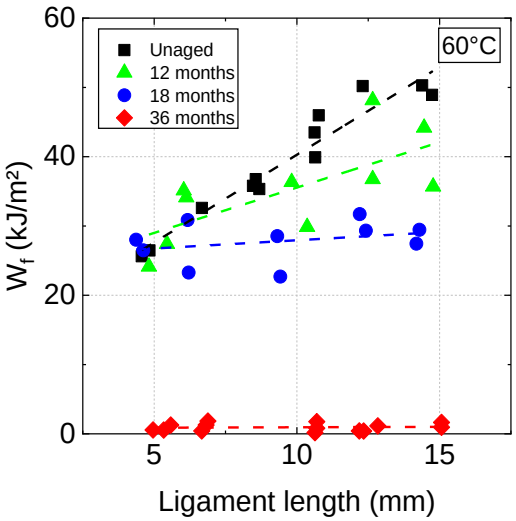

(a)

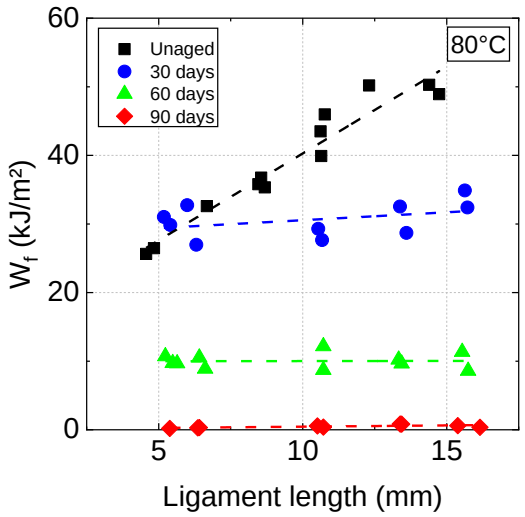

(b)

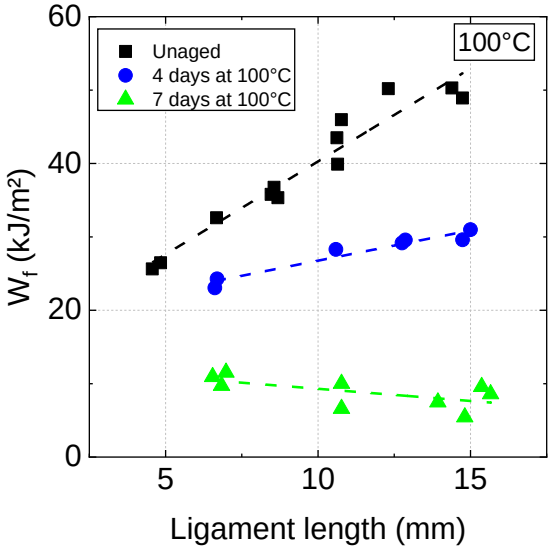

(c)

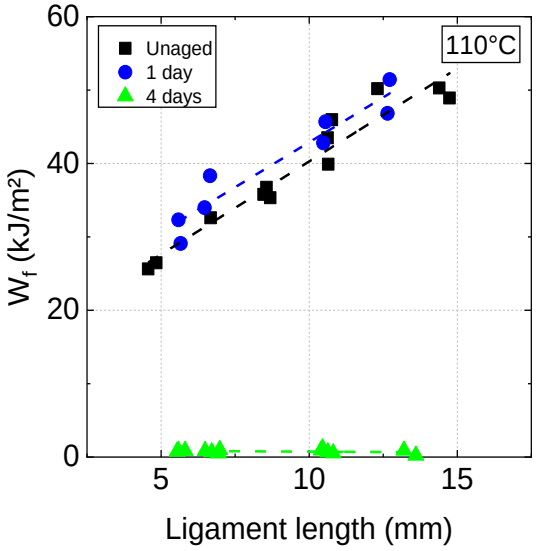

(d)

Figure 7: Effect of ligament length on fracture energy after aging performed at (a) 60°C (b) 80°C (c) 100°C (d) 110°C

From the results in Figure 7, it is clear that a common behaviour is observed for all the aging temperatures considered here. At the early stages of aging, the slope decreases slowly until it reaches a zero value for each aging temperature. After extensive degradation, the slope stays at zero value and the intercept slowly decreases until it reaches zero as well. These modifications in the fracture behaviour are clear evidence that changes are occurring upon hydrolysis and are occurring at all the aging temperatures investigated here.

Here again, it is worth noting that the fracture properties are much more sensitive to aging than those based on the maximal stress obtained from tensiles tests (see Figure 8 from [31] for comparison). For example, at 80°C with EWF-m large changes are observed in the slope (i.e. βw_p) after 30 days, whereas no change is observed in maximal stress over the first 60 days of aging. Also, while no changes are observed concerning the maximal stress at the early stages of aging, it is particularly interesting to take a look at the strain at break, known to be more sensitive but also more scattered, Figure 8.b.

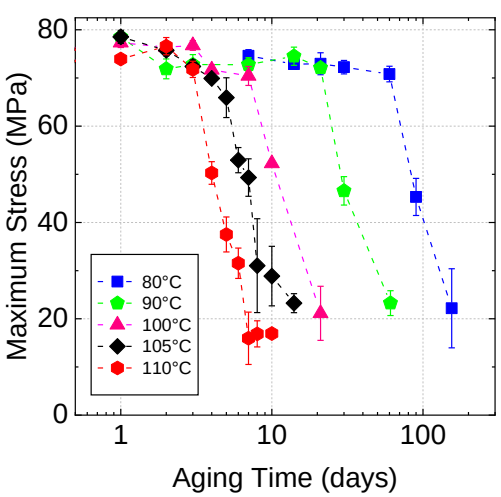

(a)

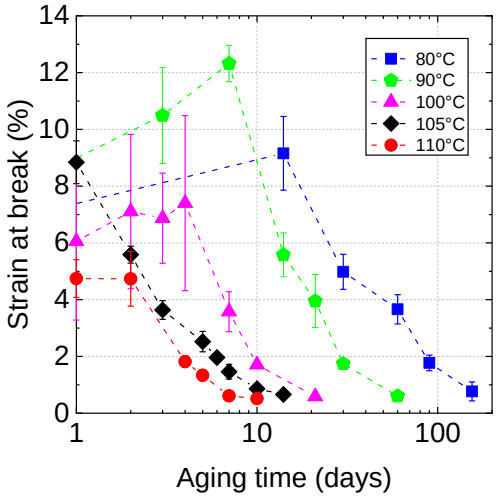

(b)

Figure 8: (a) Changes in maximum stress (from tensile tests) as a function of aging at different temperatures, from [31] (b) Changes in strain at break as a function of time

3.2.2.2. Time/Temperature superposition based on fracture properties

An important aspect is now addressed: Can the decrease in fracture properties at different temperatures be described using an Arrehnius law? If yes, how are these results relevant to existing extrapolation based on classical tensile properties? To do so, the fracture properties obtained at 105°C are used as a reference and are associated with an acceleration coefficient a_t of 1. An adjusted acceleration factor a_t is also associated with each aging temperature considered here to attempt to describe the loss in mechanical properties. Results are shown in Figure 9.a and Figure 9.b for both w_e and βw_p, respectively. The accelation factors are then found in Table 1.

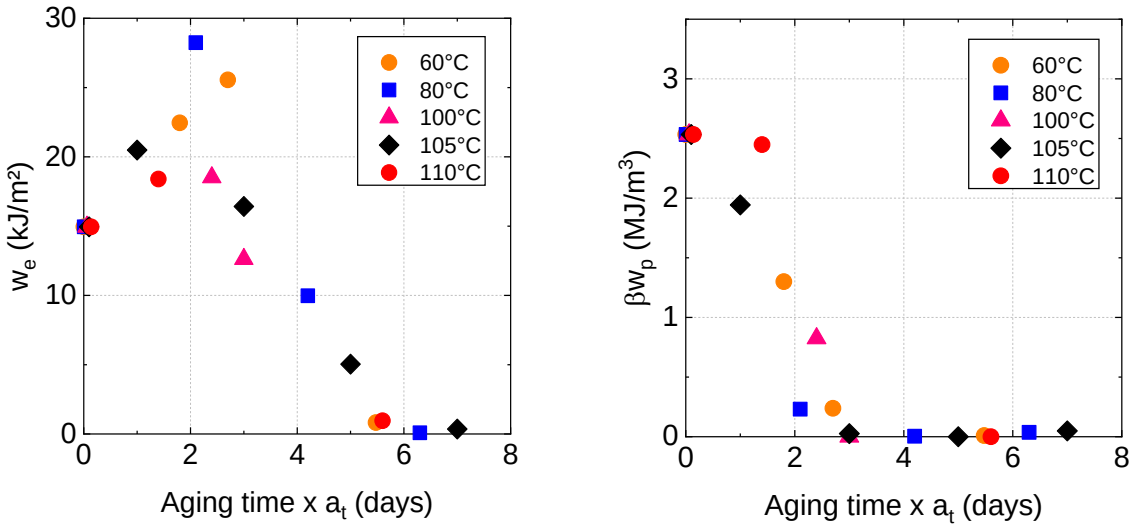

(a) **(b)**

Figure 9: Fracture properties shifted using an acceleration coefficient (a) w_e (b) βw_p

Table 1: Accelation factors for all temperatures investigated in this paper

Temperature (°C)	Acceleration factor a_t
60	0.005
80	0.07
100	0.6

105	1
110	1.4

In the same way as for the results presented in Figure 5, the trends concerning both βw_p and w_e are similar. This shows that a common behaviour is observed at all aging temperatures considered here. Figure 10 now shows an Arrhenius plot that confirms that the loss in fracture properties (both βw_p and w_e) can be described using this equation with an activation energy of 121 kJ/mol. It may be noted that this value is very close to that obtained through tensile test (115 kJ/mol) in [31] and from literature [33, 34]. At this stage, it clearly appears that using fracture properties it is possible to reduce the aging time necessary to observe a decrease in the polymer behaviour. Moreover, it has been shown that accelerating factors induced by the increase in aging temperature are the same here as those using classical tensile tests.

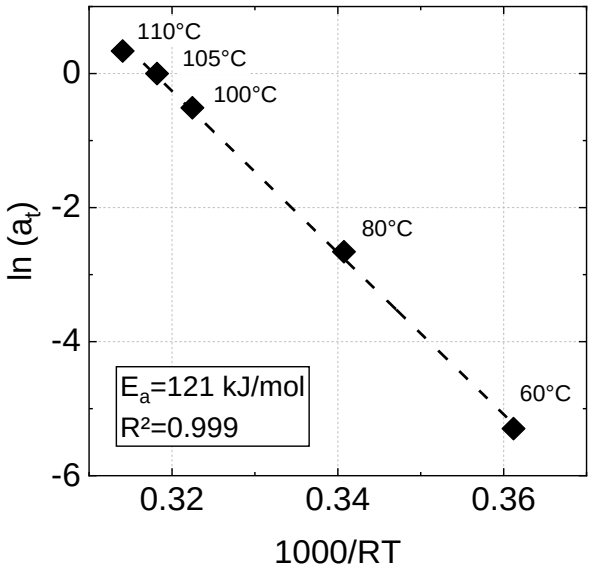

Figure 10: **Arrhenius highlighting the acceleration factors associated with fracture properties at different temperatures**

The second question that was addressed was whether it is possible to propose a relationship between the macromolecular network and the mechanical properties after aging, this is the aim of the following section.

4. Discussion - Structure/Properties relationship based on fracture properties

In PET, it is possible to describe the transition between ductile and brittle behaviour considering a critical molar mass (M'_c). If M_n is above this value, the polymer exhibits a ductile behaviour whereas if M_n is below M'_c, then the polymer is brittle [35]. The M'_c value is known for PET and is equal to 17 kg/mol [31]. In order to check whether the EWF test can be used to determine this value we first present the changes in M_n as a function of aging time for all the data points considered here, Figure 11. Results show that for a given temperature, the molar mass decreases continuously from 31 kg/mol until it reaches values close to zero. Such a result is in agreement with those in the literature [36-38]. Moreover, the lower the temperature, the slower the hydrolysis rate. This behaviour also follows an Arrhenius law. The acceleration factors were determined and were found to be very similar to those presented in Table 1.

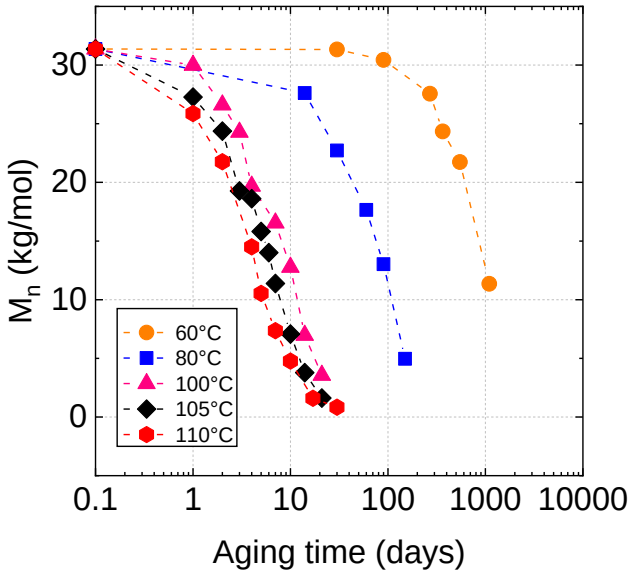

Figure 11: Effect of aging at different temperatures on the molar mass

Using data presented in Figure 7, it is possible to plot βw_p as function of M_n, see figure 12.a. βw_p is also directly compared with results from Figure 8.a concerning the maximal stress. It appears that when βw_p is above 0 then the material exhibits a ductile behaviour whereas when

βw_p is equal to 0 then the polymer is brittle. And so, it is possible to determine a value for the critical molar mass M'_c. This value is here around 17 kg/mol, i.e. in accordance with existing data in literature and results obtained considering maximal stress. However, the shapes of the two plots are quite different. On one hand, for molar masses above 17 kg/mol, the maximal stress is constant around 70 MPa while βw_p decreases linearly over the same molar mass range. On the other hand, for molar masses less than 17 kg/mol, the maximal stress decreases linearly while βw_p equals zero. In terms of methodology towards the identification of polymer embrittlement, the EWF method has a major advantage over uniaxial tensile tests. At the very early aging stages, changes in βw_p are observed while the maximal stress is constant. This means that from EWF results obtained after short aging durations, changes in βw_p can be extrapolated towards the identification of a critical molar mass. In the polymer degradation community, such a methodology is very powerful because it can significantly reduce aging duration or temperature. For example, considering EWF-m, βw_p is equal to 0 after approximately 30 days of aging at 80°C whereas it takes 75 days to observe a decrease in maximal stress using tensile tests. The same goes for aging at 60°C where brittle behaviour was observed after 20 months using EWF-m and 3 years using tensile tests. Finally, βw_p was compared with the strain at break data as a function of M_n, Figure 12.b. It appears that no clear correlation is observed, meaning that the loss in strain at break is not due to the loss in βw_p. However, as discussed in [13], the decrease in strain at break during aging may be associated with a decrease in tie molecule concentration.

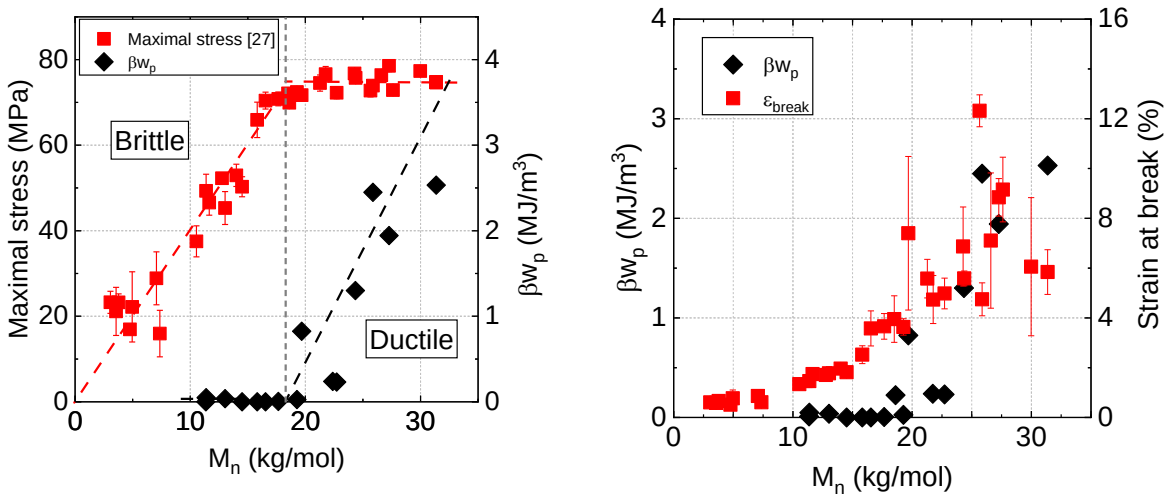

Figure 12: (a) Maximal stress (b) Strain at break from tensile tests as a function of molar mass compared with βwp as a function of molar mass

5. Conclusion

In this paper, the fracture properties of PET were investigated during hydrolytic aging using the Essential Work of Fracture at different temperatures. First, results have shown that a significant decrease in the non-essential work of fracture (βw_p) was observed during aging and that the PET exhibited a change from ductile to brittle behaviour. Second, it has been demonstrated that it was possible to identify a critical molar mass M'_c based on fracture properties. Finally, when compared to results obtained from tensile tests after aging, it was shown that the EWF test was more sensitive to aging, which could significantly reduce the time needed to age samples in durability studies. Additionally, this means that it is also possible to lower the aging temperature to temperatures closer to service temperature, which would greatly enhance the lifetime prediction.

Acknowledgments

The authors would like to thank the Microplastics project financed by Ifremer. The work of Nicolas Lacotte and Mickaël Premel-Cabic is also gratefully acknowledged.

References

[1] Planes, E., Yrieix, B., Bas, C., & Flandin, L. (2014). Chemical degradation of the encapsulation system in flexible PV panel as revealed by infrared and Raman microscopies. *Solar energy materials and solar cells*, *122*, 15-23.

[2] Le Saux, V., Le Gac, P. Y., Marco, Y., & Calloch, S. (2014). Limits in the validity of Arrhenius predictions for field ageing of a silica filled polychloroprene in a marine environment. *Polymer Degradation and Stability*, *99*, 254-261.

[3] Gillen, K. T., Bernstein, R., & Derzon, D. K. (2005). Evidence of non-Arrhenius behaviour from laboratory aging and 24-year field aging of polychloroprene rubber materials. *Polymer Degradation and Stability*, *87*(1), 57-67.

[4] Le Gac, P. Y., Albouy, P. A., Fayolle, B., & Verdu, J. (2021). Relationship between macromolecular network and fatigue properties of unfilled polychloroprene rubber. *Polymer Degradation and Stability*, *192*, 109669.

[5] Coquillat, M., Verdu, J., Colin, X., Audouin, L., & Neviere, R. (2007). Thermal oxidation of polybutadiene. Part 2: Mechanistic and kinetic schemes for additive-free non-crosslinked polybutadiene. *Polymer Degradation and Stability*, *92*(7), 1334-1342.

[6] Richaud, E., Farcas, F., Bartoloméo, P., Fayolle, B., Audouin, L., & Verdu, J. (2006). Effect of oxygen pressure on the oxidation kinetics of unstabilised polypropylene. *Polymer Degradation and Stability*, *91*(2), 398-405.

[7] Dubelley, F., Planes, E., Bas, C., Pons, E., Yrieix, B., & Flandin, L. (2018). Predictive durability of polyethylene terephthalate toward hydrolysis over large temperature and relative humidity ranges. *Polymer*, *142*, 285-292.

[8] Sang, T., Wallis, C. J., Hill, G., & Britovsek, G. J. (2020). Polyethylene terephthalate degradation under natural and accelerated weathering conditions. *European polymer journal*, *136*, 109873.

[9] Le Gac, P. Y., Celina, M., Roux, G., Verdu, J., Davies, P., & Fayolle, B. (2016). Predictive ageing of elastomers: Oxidation driven modulus changes for polychloroprene. *Polymer Degradation and Stability*, *130*, 348-355.

[10] Gillen, K. T., Celina, M., & Bernstein, R. (2003). Validation of improved methods for predicting long-term elastomeric seal lifetimes from compression stress–relaxation and oxygen consumption techniques. *Polymer Degradation and Stability*, *82*(1), 25-35.

[11] Gijsman, P., & Verdun, F. (2001). The influence of polymer type, stabilizers and sample geometry on the relationship between chemiluminescence and oxygen uptake. *Polymer degradation and stability*, *74*(3), 533-542.

[12] Gillen, K. T., Bernstein, R., Clough, R. L., & Celina, M. (2006). Lifetime predictions for semi-crystalline cable insulation materials: I. Mechanical properties and oxygen consumption measurements on EPR materials. *Polymer degradation and stability*, *91*(9), 2146-2156.

[13] Deshoulles, Q., Le Gall, M., Dreanno, C., Arhant, M., Stoclet, G., Priour, D., & Le Gac, P. Y. (2021). Origin of embrittlement in Polyamide 6 induced by chemical degradations: mechanisms and governing factors. *Polymer Degradation and Stability*, 109657.

[14] Bardin, A., Le Gac, P. Y., Cérantola, S., Simon, G., Bindi, H., & Fayolle, B. (2020). Hydrolytic kinetic model predicting embrittlement in thermoplastic elastomers. *Polymer Degradation and Stability*, *171*, 109002.

[15] Karger-Kocsis, J. (2000). Microstructural and molecular dependence of the work of fracture parameters in semicrystalline and amorphous polymer systems. In *European Structural Integrity Society* (Vol. 27, pp. 213-230). Elsevier.

[16] Moore, D. R., Williams, J. G., & Pavan, A. (2001). *Fracture mechanics testing methods for polymers, adhesives and composites*. Elsevier.

[17] Martinez, A. B., Gamez-Perez, J., Sanchez-Soto, M., Velasco, J. I., Santana, O. O., & Maspoch, M. L. (2009). The essential work of fracture (EWF) method–analyzing the post-yielding fracture mechanics of polymers. *Engineering failure analysis*, *16*(8), 2604-2617.

[18] Maspoch, M. L., Hénault, V., Ferrer-Balas, D., Velasco, J. I., & Santana, O. O. (2000). Essential work of fracture on PET films: influence of the thickness and the orientation. *Polymer testing*, *19*(5), 559-568.

[19] Mouzakis, D. E., Papke, N., Wu, J. S., & Karger-Kocsis, J. (2001). Fracture toughness assessment of poly (ethylene terephthalate) blends with glycidyl methacrylate modified polyolefin elastomer using essential work of fracture method. *Journal of applied polymer science*, *79*(5), 842-852.

[20] Bárány, T., Ronkay, F., Karger-Kocsis, J., & Czigány, T. (2005). In-plane and out-of-plane fracture toughness of physically aged polyesters as assessed by the essential work of fracture (EWF) method. *International journal of fracture*, *135*(1), 251-265.

[21] Barany, T., Czigány, T., & Karger-Kocsis, J. (2010). Application of the essential work of fracture (EWF) concept for polymers, related blends and composites: A review. *Progress in Polymer Science*, *35*(10), 1257-1287.

[22] Barany, T., Karger-Kocsis, J., & Czigany, T. (2003). Effect of hygrothermal aging on the essential work of fracture response of amorphous poly (ethylene terephthalate) sheets. *Polymer degradation and stability*, *82*(2), 271-278.

[23] Fayolle, B., Tcharkhtchi, A., & Verdu, J. (2004). Temperature and molecular weight dependence of fracture behaviour of polypropylene films. *Polymer testing*, *23*(8), 939-947.

[24] Fayolle, B., Audouin, L., & Verdu, J. (2002). Initial steps and embrittlement in the thermal oxidation of stabilised polypropylene films. *Polymer degradation and stability*, *75*(1), 123-129.

[25] Fayolle, B., Audouin, L., & Verdu, J. (2003). Radiation induced embrittlement of PTFE. *Polymer*, *44*(9), 2773-2780.

[26] McMahon, W., Birdsall, H. A., Johnson, G. R., & Camilli, C. T. (1959). Degradation Studies of Polyethylene Terephthalate. *Journal of Chemical and Engineering Data*, *4*(1), 57-79.

[27] Ballara, A., & Verdu, J. (1989). Physical aspects of the hydrolysis of polyethylene terephthalate. *Polymer Degradation and Stability*, *26*(4), 361-374.

[28] Dubelley, F., Planes, E., Bas, C., Pons, E., Yrieix, B., & Flandin, L. (2017). The hygrothermal degradation of PET in laminated multilayer. *European Polymer Journal*, *87*, 1-13.

[29] Golike, R. C., & Lasoski Jr, S. W. (1960). Kinetics of hydrolysis of polyethylene terephthalate films. *The Journal of Physical Chemistry*, *64*(7), 895-898.

[30] Pickett, J. E., & Coyle, D. J. (2013). Hydrolysis kinetics of condensation polymers under humidity aging conditions. *Polymer Degradation and Stability*, *98*(7), 1311-1320.

[31] Arhant, M., Le Gall, M., Le Gac, P. Y., & Davies, P. (2019). Impact of hydrolytic degradation on mechanical properties of PET-Towards an understanding of microplastics formation. *Polymer Degradation and Stability*, *161*, 175-182.

[32] Laun, S., Pasch, H., Longiéras, N., & Degoulet, C. (2008). Molar mass analysis of polyamides-11 and-12 by size exclusion chromatography in HFiP. *Polymer*, *49*(21), 4502-4509.

[33] Golike, R. C., & Lasoski Jr, S. W. (1960). Kinetics of hydrolysis of polyethylene terephthalate films. *The Journal of Physical Chemistry*, *64*(7), 895-898.

[34] Davies, T., Goldsmith, P. L., Ravens, D. A. S., & Ward, I. M. (1962). The kinetics of the hydrolysis of polyethylene terephthalate film. *The Journal of Physical Chemistry*, *66*(1), 175-176.

[35] Kausch, H. H. (2012). *Polymer fracture* (Vol. 2). Springer Science & Business Media.

[36] Launay, A., Thominette, F., & Verdu, J. (1999). Hydrolysis of poly (ethylene terephtalate). A steric exclusion chromatography study. *Polymer degradation and stability*, *63*(3), 385-389.

[37] Kint, D. P., de Ilarduya, A. M., & Muñoz-Guerra, S. (2003). Hydrolytic degradation of poly (ethylene terephthalate) copolymers containing nitrated units. *Polymer degradation and stability*, *79*(2), 353-358.

[38] Güçlü, G., Yalçınyuva, T., Özgümüş, S., & Orbay, M. (2003). Hydrolysis of waste polyethylene terephthalate and characterization of products by differential scanning calorimetry. *Thermochimica Acta*, *404*(1-2), 193-205.